Renewables

RESEARCH ARTICLE

Received: May 8, 2026 | Accepted: June 29, 2026 | Published: Aug. 26, 2026

Electrochemically Mediated Chemical Tandem Catalysis for Dimethyl Carbonate Electrosynthesis from CO_2 and Methanol

Zifeng Wu[1], Weixiang Xiong[2], Guangxing Yang[2]*, Hao-Fan Wang[1], Yonghai Cao[1], Hongjuan Wang[1]*, Hao Yu[1] & Feng Peng[2]*

[1]*School of Chemistry and Chemical Engineering, South China University of Technology, Guangzhou 510641* , [2]*School of Chemistry and Chemical Engineering, Guangzhou University, Guangzhou 510006*

[*]*Corresponding authors: yanggx@gzhu.edu.cn; cehjwang@scut.edu.cn; fpeng@gzhu.edu.cn*

Cite this: *Renewables* **2026**, 4, 183–188
DOI: 10.31635/renewables.026.202600119

An electrochemically mediated chemical tandem catalysis strategy is reported for the efficient electrosynthesis of dimethyl carbonate (DMC) directly from CO_2 and methanol. Herein, we report a tandem electrochemical system comprising cathodic CO_2 reduction to CO and anodic methanol oxidation, connected by gas transfer, achieving a stable DMC faradaic efficiency of 72% over 10 h. Mechanistic studies provide the first direct evidence of methoxy radical ($\bullet OCH_3$) generation at the anode during methanol oxidation and, more importantly, the unprecedented verification of its redox interaction with Br^- anions. In addition, the Br^-/Br_2 redox shuttle acts as both electron carrier and mediator for catalyst regeneration. This chemical tandem pathway enables efficient Pd^{2+} catalyst cycling without external oxidants, achieving sustainable DMC production. The integrated approach not only circumvents the thermodynamic limitations of direct CO_2-methanol carbonylation but also establishes a general paradigm for electrochemical tandem catalysis by decoupling electron transfer and catalytic turnover.

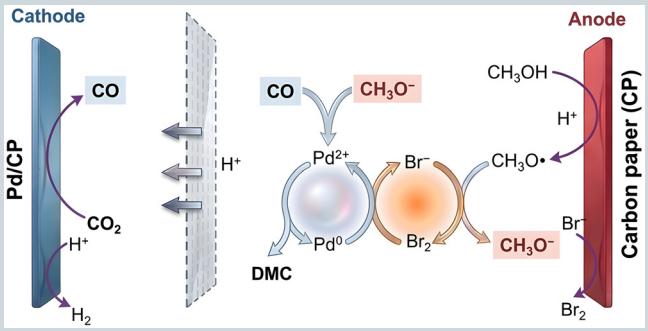

Keywords: CO_2 electroreduction, electrosynthesis, dimethyl carbonate, methanol electroxidation, electrocatalysis

Introduction

Dimethyl carbonate (DMC) is a green chemical with widespread applications as a fuel additive,[1–3] lithium battery solvent,[4–6] and polycarbonate monomer.[7–9] Current industrial production relies on oxidative carbonylation of methanol using toxic CO/NO_x mixtures under high-temperature/pressure conditions,[10,11] raising safety and environmental concerns. Electrochemistry and electrocatalysis are gaining increasing attention in the fields of energy conversion and synthesis.[12–16] Electrochemical synthesis of DMC from CO_2 and methanol offers a promising alternative under ambient conditions. This route can directly harness renewable electricity, enabling energy-efficient conversion with a minimal carbon footprint. More broadly, it falls under the umbrella of CO_2 electroreduction, a rapidly advancing field that converts greenhouse gas into valuable chemicals using only electrons as the reducing agent.[17,18] By integrating CO_2 fixation with methanol activation, electrosynthesis of DMC avoids hazardous oxidants and high-pressure gas feeds, simplifies process safety, and lowers equipment costs. As such, electrochemical strategies are increasingly recognized as a sustainable and powerful platform for chemical synthesis, aligning with green chemistry principles and the global shift toward electrically driven chemical manufacturing.[19–22]

Recent progress has demonstrated three major strategies for DMC electrosynthesis: (1) anodic oxidative carbonylation using CO gas over Pd-based catalysts (FE up to 93%);[23–25] (2) redox-neutral solution-phase coupling in undivided cells (FE 60–80%);[26–28] and

(3) direct cathodic surface coupling (FE 47.5–52.3%).[29,30] Despite these advances, the fundamental mechanism, particularly the nature of methoxy intermediates and their coupling pathways, remains a subject of debate. Surface-adsorbed CH_3O^* species have been detected on Pd-based anodes, while solution-phase Pd(II)-CO complexes are proposed for redox-neutral systems. However, direct evidence for methoxy radical ($CH_3O•$) intermediates, which could bridge these mechanisms, has been elusive.

Herein, we design a tandem electrochemical system composed of a separated two-compartment H-type cell configuration where cathodic CO_2 reduction to CO is physically connected to anodic methanol oxidation via gas transfer. This H-type cell configuration decouples the two reactions while enabling efficient CO delivery. Remarkably, mechanistic studies using radical trapping experiments reveal a free-radical-mediated pathway: methanol undergoes direct anodic oxidation to generate $CH_3O•$ radicals, which subsequently oxidize bromide (Br^-) to bromine (Br_2) and are reduced to CH_3O^-. The CH_3O^- then couples with CO over Pd^{2+} catalysts to produce DMC, completing a tandem catalytic cycle. This work establishes the role of $CH_3O•$ radicals as critical intermediates bridging anodic oxidation and carbonylation, opening new avenues for designing tandem electrochemical systems.

Results and discussion

Tandem electrochemical system design and performance evaluation

To investigate the role of cell configuration on DMC electrosynthesis, we constructed and compared two electrochemical systems: a one-compartment undivided cell and a two-compartment divided cell separated by a Nafion membrane (Figure 1a and c). In the one-compartment cell, both electrodes were immersed i n a methanol electrolyte containing KBr and $PdBr_2$ with continuous CO_2 purging. Under cathodic potential, DMC formation in the electrolyte was confirmed by ^1H NMR (Supporting Information Figure S1) spectroscopy, ^{13}C NMR spectroscopy (Supporting Information Figure S2), and gas chromatogram-mass spectrometry (Supporting Information Figure S3). The quantity of CO, H_2, and DMC was determined by GC via calibration curves (Supporting Information Figure S4). However, the faradaic efficiency for DMC decreased progressively from 60% to 30% over 8 h of electrolysis (Figure 1b). Concurrently, the Pd^{2+} concentration in the electrolyte declined from 0.78 to 0.1 mM (Figure 1b). Postelectrolysis characterization revealed metallic Pd deposits on the cathode surface (Supporting Information Figure S5), indicating that Pd^{2+} species migrated to the cathode and were electrochemically reduced. This Pd^{2+} depletion accounts for the declining DMC efficiency, as Pd^{2+} serves as the essential homogeneous catalyst for carbonylation.

To prevent Pd^{2+} reduction at the cathode and maintain catalytic activity, we designed a two-compartment cell with physical separation of the anode and cathode (Figure 1c). The cathodic compartment contained a home-made Pd/CP electrode (Supporting Information Figure S6–S9) in methanol with KBr electrolyte, continuously purged with CO_2. The anodic compartment contained a carbon paper electrode in methanol with KBr electrolyte and $PdBr_2$ catalyst. Critically, CO gas generated at the cathode from CO_2 reduction (Supporting Information Figure S10) was delivered through a connecting tube to the anodic chamber, enabling tandem coupling while preventing Pd^{2+} migration to the cathodic compartment. Through optimizing the reaction conditions, the cathode and proton exchange membrane (Supporting

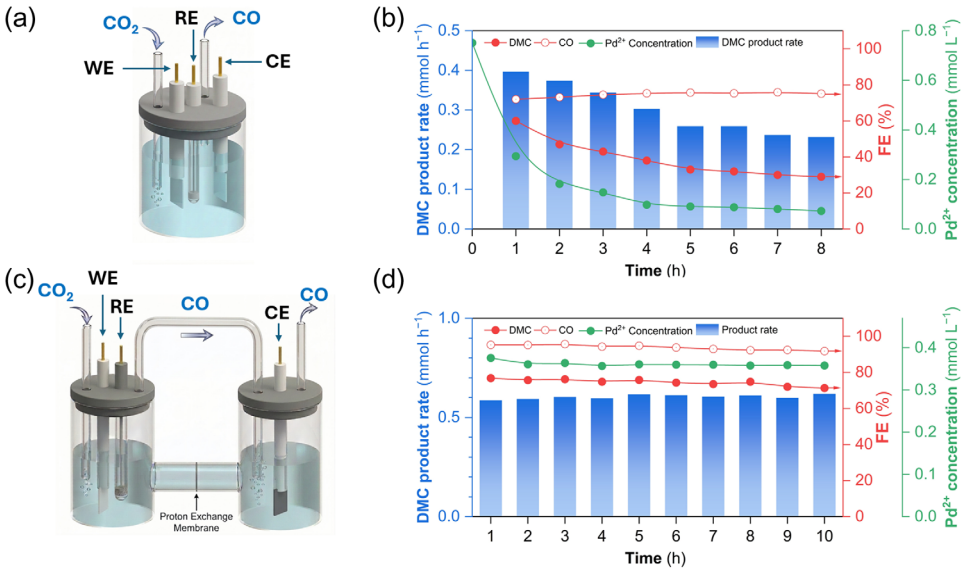

Figure 1 | *DMC electrosynthesis via one-compartment and two-compartment electrochemical cells. (a) One-compartment and (c) two-compartment cell for electrochemical synthesis of DMC. DMC production rate, faradaic efficiency, and Pd^{2+} concentration as a function of electrolysis time in the (b) one-compartment cell and (d) two-compartment cell. The potential is applied to the cathode.*

DOI: 10.31635/renewables.026.202600119
Citation: *Renewables* **2026**, 4, 183–188
Link to VoR: https://doi.org/10.31635/renewables.026.202600119

Table 1 | *DMC Detection Under Various Conditions.*

Entry	Conditions	Potential	DMC
1	0.1 M KBr-CH_3OH	YES	NO
2	0.1 M KBr-CH_3OH + $PdBr_2$	YES	NO
3	0.1 M KBr-CH_3OH + CO	YES	NO
4	0.1 MKBr-CH_3OH (Blank electrolyte, no CH_3O^-) + $PdBr_2$ + CO	NO	NO
5	CH_3OK + Pd powder + CO	NO	NO
6	0.1 M KBr-CH_3OH + $PdBr_2$ + CO	YES	YES
7	Entry 2 without CO_2	YES	NO
8	CH_3OH + $PdBr_2$ + CO	YES	NO
9	0.1 M KBr-CH_3OH + $PdBr_2$ + CO	Open-circuit	NO

Information Figure S11–S14), the two-compartment cell achieved a stable DMC faradaic efficiency of 72% at 47 mA cm^{-2} over 10 h of continuous operation (Figure 1d). Cathodic CO production maintained 92% faradaic efficiency throughout the electrolysis, confirming efficient CO_2 reduction. The DMC production rate reached 308 μmol h^{-1} mg_{Pd}^{-1}, with a cumulative DMC yield of approximately 6.19 mmol within this period, outperforming previously reported systems (Supporting Information Figures S15 and S16 and Table S1). Notably, the Pd^{2+} concentration in the anolyte remained constant during the 10 h electrolysis (Figure 1d), demonstrating that physical separation effectively prevented Pd^{2+} reduction and deposition at the cathode.

This stability directly correlates with the sustained DMC faradaic efficiency. The cathode material of Pd/CP after long-term operation remains unchanged (Supporting Information Figures S17 and S18). In our validation experiments, no significant Pd migration, deposition, or loss was observed after long-term electrolysis (Supporting Information Figure S19 and Tables S2 and S3). The contrasting performance between single- and two-compartment cells highlights a critical design principle for tandem electrochemical systems: spatial separation of the catalyst (Pd^{2+}) from the reducing environment of the cathode is essential for long-term stability.

Identification of essential reaction components

A systematic investigation was conducted to verify the mechanism of DMC synthesis using 0.1 M KBr-CH_3OH electrolyte (Table 1 and Supporting Information Figure S20) in the two-compartment cell (Figure 1c). Experimental data show that Entries 1–3 from the individual tests of the anolyte, addition of $PdBr_2$, or CO introduction, all yielded no DMC. Entry 4, combining $PdBr_2$ and CO in blank electrolyte (no CH_3O^-) without applied potential, also failed to produce DMC. Entry 5 employed CH_3OK as the CH_3O^- source with Pd powder and CO without external potential, yet no DMC was detected. Only Entry 6, in which $PdBr_2$ and CO were introduced into the anolyte under an applied potential of −3.0 V vs Ag/Ag^+ in cathode, successfully yielded DMC.

Logical analysis of these results reveals three critical requirements. First, the absence of DMC in Entry 4 demonstrates that CH_3O^- is an indispensable nucleophilic precursor, even when both Pd^{2+} catalyst and CO are present. Second, the negative result in Entry 3 contrasts sharply with the positive outcome in Entry 6, confirming that Pd^{2+} catalytic species are essential for activating the C–O bond formation pathway. Furthermore, Entries 5 and 6 reveal that the catalytic active species of Pd for the carbonyl reaction is Pd^{2+}, rather than Pd^0: although both experiments contained CH_3O^-, Pd species, and CO, DMC was synthesized only under Pd^{2+} conditions. Third, the comparison between Entries 2 and 6 establishes CO as the necessary carbonyl source for DMC formation. Additionally, the results of Entries 2–3 and 7–9 eliminate background reactions or other side reactions as potential sources of DMC formation. Therefore, DMC synthesis under these conditions requires three essential elements: (1) CH_3O^- as the nucleophilic precursor; (2) Pd^{2+} catalytic species for reaction activation; and (3) CO as the carbonyl source. All three components are strictly necessary and must work synergistically to achieve efficient DMC synthesis.

Anodic detection of methoxy radicals and their redox interaction with bromide

In an anodic electrolytic cell containing 0.1 M KBr-CH_3OH and $PdBr_2$ under constant applied potential, a distinct color transition from brown to bright yellow was observed, accompanied by the characteristic blue coloration of starch-iodide paper, unequivocally confirming the generation of Br_2 (Supporting Information Figures S21 and S22). Concurrently, the introduction of *tert*-butyl iodide during electrolysis resulted in the gas chromatographic (GC) detection of methyl *tert*-butyl ether, providing indirect evidence for the presence of CH_3O^- in the reaction system (Figure 2a).

To elucidate the origin of these methoxide anions, a series of controlled experiments were conducted. In a 0.1 M $NaBF_4$-CH_3OH electrolytic system, electron paramagnetic resonance (EPR) spectroscopy unambiguously detected characteristic signals of methoxy radicals (CH_3O•), representing the first experimental confirmation of CH_3O• generation at the anode during electrochemical methanol oxidation (Figure 2b) with DMPO (5,5-Dimethyl-1-pyrroline N-oxide) as trapping agent. Furthermore, in the absence of Br^-, methyl *tert*-butyl ether was not detected, indicating the absence of CH_3O^- anion formation (Supporting Information Figure S23) after which no DMC was detected (Figure 2c). Remarkably, the addition of Br^- to the postelectrolysis solution resulted in the development of a blue coloration with starch-iodide reagent, demonstrating that Br_2 was indeed generated during the reaction (Figure 2d), and CH_3O^- was detected again (Supporting Information Figure S24).

These experimental phenomena reveal crucial mechanistic insights. Br^- anions not only undergo anodic oxidation to Br_2 but also participate as redox mediators in the conversion of CH_3O• radicals to CH_3O^- anions. When the electrolyte KBr was replaced with nonhalide salts such as $NaBF_4$, no DMC was detected (Figure 2c). Concurrently, the appearance of black particulates was observed (Figure 2e), confirming that Pd^{2+} was reduced to metallic Pd^0 by CO, resulting in catalytic cycle

DOI: 10.31635/renewables.026.202600119
Citation: *Renewables* **2026**, 4, 183–188
Link to VoR: https://doi.org/10.31635/renewables.026.202600119

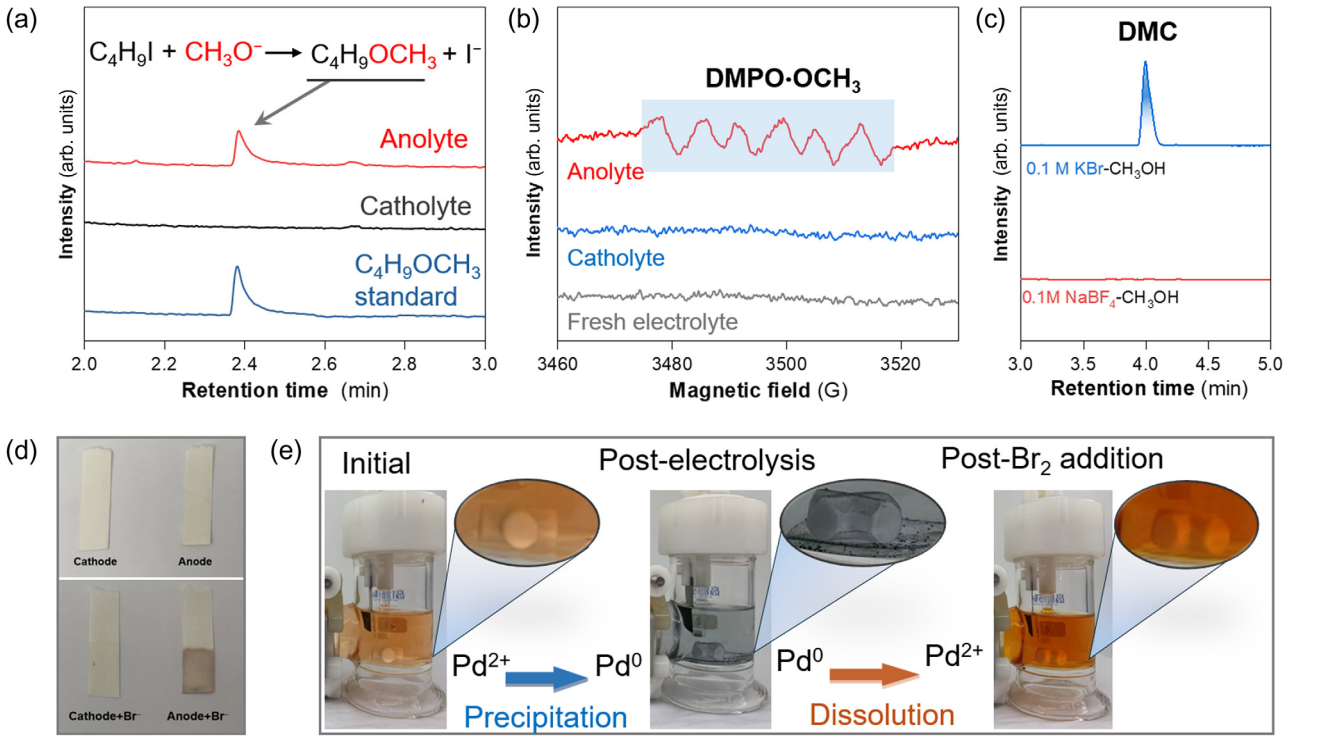

Figure 2 | *Mechanistic investigation of $CH_3O•/CH_3O-$ interconversion and their redox interaction with bromine species during electrosynthesis. (a) GC analysis of n-butyl iodide trapping experiment. (b) EPR spectra using DMPO as a spin-trapping agent. (c) GC detection of DMC formation in different electrolyte systems. (d) Colorimetric analysis using starch–iodide paper to verify the formation of Br_2. (e) Photos of the electrolyte prior to (left), after (middle) electrolysis in 0.1 M $NaBF_4$–CH_3OH, and after Br_2 addition into the postelectrolysis electrolyte (right).*

interruption in the absence of Br^- anions. The subsequent addition of Br_2 to the deactivated system resulted in the disappearance of black precipitates and the restoration of the characteristic color of Pd^{2+} solution (Figure 2e), Importantly, ICP analysis revealed that the dissolved Pd concentration returned to a value close to its initial level after the addition of Br_2 (Supporting Information Table S4), demonstrating that Br_2 reoxidized Pd^0 back to Pd^{2+}, thereby achieving the regeneration of the catalytic cycle.

Electrochemically mediated chemical tandem catalysis

Based on the comprehensive experimental evidence described above, the formation mechanism of DMC can be rationally derived through the following five fundamental steps as shown in Figure 3. First, methanol undergoes direct electrochemical oxidation at the anode surface, losing one electron to generate $CH_3O•$ radicals and H^+ ($CH_3OH \rightarrow CH_3O• + e^- + H^+$). Second, $CH_3O•$ radicals, acting as strong oxidants, oxidize Br^- in the solution to Br_2 while they accept electrons and are reduced to CH_3O^- ($2CH_3O• + 2Br^- \rightarrow Br_2 + 2CH_3O^-$). This step represents the first experimental verification of the redox interaction between methoxy radicals and bromide ions, confirmed by the EPR detection of methoxy radicals captured by DMPO, the absence of methoxide anions without Br^-, and the detection of Br_2 and CH_3O^- after the addition of Br^-. Third, Pd^{2+} undergoes ligand exchange with methoxide anions to form dimethoxy palladium (II) complexes ($PdBr_2 + 2CH_3O^- \rightleftharpoons [Pd(OCH_3)_2] + 2Br^-$) and a CO molecule inserts into the Pd-O bond, forming a palladium-acyloxy intermediate ($[Pd(OCH_3)_2] + CO \rightarrow [Pd\text{-}C(O)OCH_3] + CH_3O^-$).[26] Fourth, $[Pd\text{-}C(O)OCH_3]$ is attacked by free CH_3O^- anions, generating DMC and reducing Pd^{2+} to Pd^0 ($[Pd\text{-}C(O)OCH_3] + CH_3O^- \rightarrow (CH_3O)_2C=O + Pd^0$).[26] Finally, the Br_2 generated in step 2 acts as an oxidant to reoxidize Pd^0 back to Pd^{2+} ($Pd^0 + Br_2 \rightarrow PdBr_2$), thereby achieving catalyst recycling. The core of this mechanism lies in a

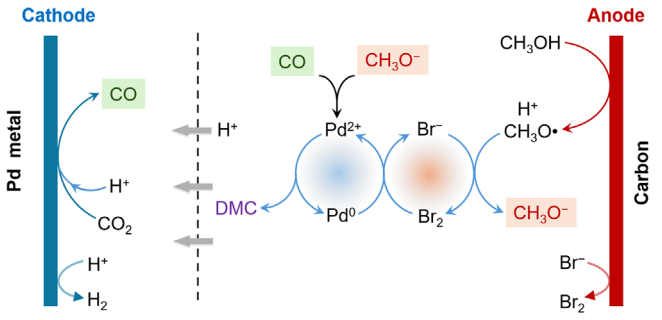

Figure 3 | *Schematic of electrochemical and chemical catalytic reactions during DMC synthesis in a separated two-compartment cell.*

DOI: 10.31635/renewables.026.202600119
Citation: *Renewables* **2026**, 4, 183–188
Link to VoR: https://doi.org/10.31635/renewables.026.202600119

dual role of the Br^-/Br_2 redox couple. On one hand, it accepts electrons from $\bullet OCH_3$ radicals to generate Br_2 while simultaneously reducing $\bullet OCH_3$ radicals to CH_3O^- anions. On the other hand, it reoxidizes the reduced Pd^0 back to Pd^{2+}, ensuring the sustainability of the catalytic cycle. The complete catalytic cycle can be summarized by the overall reaction: $2CH_3OH + CO_2 \rightarrow (CH_3O)_2C{=}O + H_2O$. This mechanistic elucidation, particularly the pioneering detection of methoxy radicals at the anode and the demonstration of their redox interaction with bromide ions, provides critical theoretical insights for the rational design of catalysts and process optimization in electrochemical carbonylation reactions.

Conclusion

In summary, we have developed a novel electrochemically mediated chemical tandem catalysis system for efficient DMC production directly from CO_2 and methanol, achieving 72% faradaic efficiency with stable performance over 10 h. The key mechanistic breakthrough lies in the first direct detection of methoxy radicals at the anode and the unprecedented verification of their redox interaction with bromide ions. This free-radical-mediated pathway enables efficient coupling between anodic methanol oxidation and cathodic CO_2 reduction, with Br^-/Br_2 serving as a pivotal redox shuttle that simultaneously regenerates Pd^{2+} catalysts and eliminates the need for external oxidants. By decoupling electron transfer from catalytic turnover, this work establishes a general paradigm for designing tandem electrochemical systems that overcome thermodynamic limitations of direct CO_2 utilization. These findings not only advance the fundamental understanding of radical-mediated electrochemical processes but also provide critical insights for developing sustainable CO_2 utilization strategies in industrial applications.

Supporting Information

Supporting Information is available and includes characterization, electrochemistry, and calculations.

Conflict of Interest

There is no conflict of interest to report.

Funding Information

This work was supported by the National Natural Science Foundation of China (grant nos. 22008076 and 22272038).

References

1. Amine, M.; Barakat, Y. Effect of Dimethyl Carbonate Addition on Ethanol–Gasoline Fuel Blend. *Sci. Rep.* **2023**, *13*, 14551.
2. Pacheco, M. A.; Marshall, C. L. Review of Dimethyl Carbonate (DMC) Manufacture and its Characteristics as a Fuel Additive. *Energy & Fuels* **1997**, *11*, 2–29.
3. Maier, T.; Härtl, M.; Jacob, E.; Wachtmeister, G. Dimethyl Carbonate (DMC) and Methyl Formate (MeFo): Emission Characteristics of Novel, Clean and Potentially CO_2-Neutral Fuels Including PMP and sub-23 nm Nanoparticle-Emission Characteristics on a Spark-Ignition DI-Engine. *Fuel* **2019**, *256*, 115925.
4. Li, Y.; Wang, Z.; Lin, W.; Wei, B.; Chen, D. A Concentrated Electrolyte of LiTFSI and Dimethyl Carbonate for High-Voltage Li Batteries. *ACS Appl. Energy Mater.* **2023**, *6*, 9337–9346.
5. Zhang, X.; Xu, P.; Duan, J.; Lin, X.; Sun, J.; Shi, W.; Xu, H.; Dou, W.; Zheng, Q.; Yuan, R. A Dicarbonate Solvent Electrolyte for High Performance 5 V-Class Lithium-Based Batteries. *Nat. Commun.* **2024**, *15*, 536.
6. Parhizi, M.; Caceres-Martinez, L. E.; Modereger, B. A.; Kenttämaa, H. I.; Kilaz, G.; Ostanek, J. K. Determining the Composition of Carbonate Solvent Systems used in Lithium-Ion Batteries Without Salt Removal. *Energies* **2022**, *15*, 2805.
7. Fang, W.; Zhang, Z.; Yang, Z.; Zhang, Y.; Xu, F.; Li, C.; An, H.; Song, T.; Luo, Y.; Zhang, S. One-Pot Synthesis of Bio-Based Polycarbonates from Dimethyl Carbonate and Isosorbide Under Metal-Free Condition. *Green Chem.* **2020**, *22*, 4550–4560.
8. Zeng, C.; Zhang, S.; Ji, P.; Qiu, Z.; Li, Z.; Wang, C.; Wang, H. Facile Sustainable Synthesis of Polyester-Polycarbonate and Effects of the Carbonate on Thermal, Mechanical, and Transparency Properties. *ACS Sustain. Chem. Eng* **2023**, *11*, 15754–15764.
9. Fang, W.; Zhang, Y.; Yang, Z.; Zhang, Z.; Xu, F.; Wang, W.; He, H.; Diao, Y.; Zhang, Y.; Luo, Y. Efficient Activation of Dimethyl Carbonate to Synthesize Bio-Based Polycarbonate by Eco-Friendly Amino Acid Ionic Liquid Catalyst. *Appl. Catal. A: Gen.* **2021**, *617*, 118111.
10. Wang, D.; Shi, F.; Wang, L. A Review of Catalysts for Synthesis of Dimethyl Carbonate. *Catalysts* **2024**, *14*, 259.
11. Peng, L.; Song, W.; Ren, J. Advances in Study on Methanol Oxidative Carbonylation to Dimethyl Carbonate. *ChemCatChem* **2025**, *17*, e202401528.
12. Zhang, B.; Chen, J.-Q.; Chen, J.; Yang, G.; Zhang, Q.; Liu, Z.; Peng, F. Regulating Flux-Induced Kinetic Poisoning for Ampere-Scale Current Density in Alcohol Electrooxidation. *ACS Energy Lett.* **2026**, *11*, 4980–4987.
13. Yang, G.; Chen, J.; Chen, J.; Liu, D.; Yuan, J.; Wu, Z.; Liu, Z.; Zhang, Q.; Yu, H.; Peng, F. Influence of Diffusion Field Alterations on Reactant and Intermediate Adsorption in Oxygen Reduction Pathways. *Adv. Energy Mater.* **2025**, *15*, 2500558.
14. Wu, Z.; Yang, G.; Zhang, Q.; Liu, Z.; Peng, F. Deciphering the High Overpotential of the Oxygen Reduction Reaction via Comprehensively Elucidating the Open Circuit Potential. *Energy & Environ. Sci.* **2024**, *17*, 3338–3346.
15. Leech, M. C.; Garcia, A. D.; Petti, A.; Dobbs, A. P.; Lam, K. Organic Electrosynthesis: from Academia to Industry. *React. Chem. Eng.* **2020**, *5*, 977–990.
16. Brachi, M.; El Housseini, W.; Beaver, K.; Jadhav, R.; Dantanarayana, A.; Boucher, D. G.; Minteer, S. D. Advanced Electroanalysis for Electrosynthesis. *ACS Org. Inorg. Au* **2024**, *4*, 141–187.
17. Zhou, Z.-G.; Zhang, J.; Xie, Q.; Li, J.; Xu, P.-P.; Zhang, X.-F.; Du, Z.-Y.; He, C.-T.; Chen, X.-M. A N-Heterocyclic Olefin Decorated Organic–Inorganic Dual-Site Catalyst Toward Multiple Component CO_2 Fixation. *Renewables* **2024**, *2*, 405–413.
18. Guo, M.; Cao, G.; He, X.; Yang, G.; Wang, H.; Zhang, Q.; Liu, Z.; Peng, F. 100 Gram-Scale Organic-Free Synthesis of $Bi_2O_2CO_3$

DOI: 10.31635/renewables.026.202600119
Citation: *Renewables* **2026**, 4, 183–188
Link to VoR: https://doi.org/10.31635/renewables.026.202600119

Nanosheets for Highly Selective Formate Production in CO_2 Electroreduction. *J. Mater. Chem. A* **2025**, *13*, 37942–37952.
19. Möhle, S.; Zirbes, M.; Rodrigo, E.; Gieshoff, T.; Wiebe, A.; Waldvogel, S. R. Modern Electrochemical Aspects for the Synthesis of Value-Added Organic Products. *Angew. Chem. Int. Ed.* **2018**, *57*, 6018–6041.
20. Pollok, D.; Waldvogel, S. R. Electro-Organic Synthesis – A 21st Century Technique. *Chem. Sci.* **2020**, *11*, 12386–12400.
21. Zhou, C.; Chen, J.; Zhao, J.; Meng, Y.; Li, Z.; Meng, X.; Wang, J. Glycerol Electrooxidation to Value-Added C_1–C_3 Chemicals: Mechanism Analyses, Influencing Factors, Catalytic Regulation, and Paired Valorization. *Renewables* **2024**, *2*, 89–110.
22. Fu, X.; Pedersen, J. B.; Zhou, Y.; Saccoccio, M.; Li, S.; Sa inas, R.; Li, K.; Andersen, S. Z.; Xu, A.; Deissler, N. H.; Mygind, J. B. V.; Wei, C.; Kibsgaard, J.; Vesborg, P. C. K.; Nørskov, J. K.; Chorkendorff, I. Continuous-Flow Electrosynthesis of Ammonia by Nitrogen Reduction and Hydrogen Oxidation. *Science* **2023**, *379*, 707–712.
23. Shi, Y.; Hu, Y. F.; Ye, J.; Zhong, G.; Xia, C.; Liu, Z. P.; Huang, Y.; He, L., Stabilization of Pd^0 by Cu Alloying: Theory-Guided Design of Pd^3Cu Electrocatalyst for Anodic Methanol Carbonylation. *Angew. Chem.* **2024**, *136*, e202401311.
24. Zhuang, T.-T.; Nam, D.-H.; Wang, Z.; Li, H.-H.; Gabardo, C. M.; Li, Y.; Liang, Z.-Q.; Li, J.; Liu, X.-J.; Chen, B. Dopant-Tuned Stabilization of Intermediates Promotes Electrosynthesis of Valuable C_3 Products. *Nat. Commun.* **2019**, *10*, 4807.
25. Mi, Y.; Xue, Y.; Yan, Y.; Hao, S.; Hu, C.; Zhang, L.; Zheng, G. Promoting Intermediate Stabilization and Coupling for Dimethyl Carbonate Electrosynthesis. *Small* **2025**, *21*, 2501780.
26. Lee, K. M.; Jang, J. H.; Balamurugan, M.; Kim, J. E.; Jo, Y. I.; Nam, K. T. Redox-Neutral Electrochemical Conversion of CO_2 to Dimethyl Carbonate. *Nat. Energy* **2021**, *6*, 733–741.
27. Li, X.; Han, S.-G.; Wu, W.; Zhang, K.; Chen, B.; Zhou, S.-H.; Ma, D.-D.; Wei, W.; Wu, X.-T.; Zou, R. Convergent paired Electrosynthesis of Dimethyl Carbonate from Carbon Dioxide Enabled by Designing the Superstructure of Axial Oxygen Coordinated Nickel Single-Atom Catalysts. *Energy Environ. Sci.* **2023**, *16*, 502–512.
28. Han, S.-G.; Zhou, S.; Li, X.; Zhao, J.; Wei, W.-B.; Zheng, L.; Ma, D.-D.; Wu, X.-T.; Zhu, Q.-L. Structure-Induced Interfacial Activation Convoying the CO-Relayed Conversion of CO_2 to Dimethyl Carbonate. *Chem. Eng. J.* **2024**, *486*, 150179.
29. Wang, K.-A.; Wang, Z.-L.; Hu, H.-C.; Zhu, H.-B.; Yang, H. Single B-Doped Palladium Electrocatalyst Enabling Direct Cathodic Coupling of Carbon Dioxide with Methanol into Dimethyl Carbonate. *Chem. Eng. J.* **2024**, *498*, 155109.
30. Guan, X.-H.; Wang, K.-A.; Wang, Z.-L.; Hu, H.-C.; Feng, B.; Yang, L.-J.; Zhu, H.-B.; Yang, H. Au Atom Tailoring of Palladium Nanocatalysts to Boost Cathodic Coupling of Carbon Dioxide and Methanol into Dimethyl Carbonate. *J. Mater. Chem. A* **2025**, *13*, 18367–18377.

DOI: 10.31635/renewables.026.202600119
Citation: *Renewables* **2026**, 4, 183–188
Link to VoR: https://doi.org/10.31635/renewables.026.202600119